# Achievable Rate Region for Wireless Multiple Access Channels with UAV Relay and k Independent Transmitters

Padideh Nobakht[1], Amir Masoud Aminian Modarres[*2], Ghosheh Abed Hodtani[3]

[1]Dr, Department of Electrical Engineering, sadjad University, Mashhad, Iran
[2]Dr, Department of Electrical Engineering, sadjad University, Mashhad, Iran
[3]Profssor, Department of Electrical Engineering, Ferdowsi University, Mashhad, Iran

**Abstract:**

This paper considers and characterizes a multiple access relay channel (MARC) with $k$ transmitters, one UAV relay, and a terrestrial receiver, where we derive a new achievable rate region for the continuous alphabet wireless with an unmanned aerial vehicle (UAV) relay. The derived rate region is then evaluated numerically and compared with those of multiple access channels (MAC) and MARC with terrestrial relays. The results show that the presence of a UAV relay increases the achievable rate region of MAC systems by exploiting higher line-of-sight (LoS) channel quality and time-varying spatial link gains due to the UAV's position. This improvement in the achievable region is not merely due to the UAV's presence but arises from the different channel geometry and dynamic link conditions introduced by the UAV relay compared with terrestrial relays.

**Keywords:**

achievable rate region, multiple access relay channel, UAV.

[*] Email: am_aminian@sadjad.ac.ir

AUT Journal of Electrical Engineering
10.22060/EEJ.2026.23943.5643

## 1. Introduction

As mobile communication systems continue to expand, the development of new methods to enhance network capacity has become essential. MAC and MARC are among the key technologies that can improve coverage, achievable rate regions, and rates. On the other hand, the integration of UAVs into multiple access channels enables the establishment of fast and efficient emergency networks, offering high maneuverability (ability to be placed in any desired location and height) and low deployment costs [1, 2, 3, 4, 5], which fundamentally alters the wireless channel geometry compared to terrestrial settings. Therefore, the presence of UAVs in multiple access channels makes it possible to have a fast and efficient emergency network. Additionally, due to their low energy consumption, high mobility, wide coverage, low delay, and comparative coverage, UAVs are expected to play a significant role in the future of telecommunications [1, 2, 3, 4, 5].

In most wireless communication systems, a key characteristic is the absence of a direct line of sight between transmitters and receivers, leading to random variations in the channel coefficients, a phenomenon known as channel fading. To mitigate fading effects, more sophisticated and sometimes nonlinear signal processing techniques are often required at the transmitter and receiver, increasing system cost and latency [6, 7, 8, 9, 10]. One of the major advantages of UAVs is that they can often establish a direct line of sight between the transmitter and the receiver. As a result, the channel coefficients are often less random and more predictable than typical terrestrial fading environments, which simplifies estimation and exploitation of link quality.

Because the channel coefficients depend on the UAV's spatial position, the achievable rate region also becomes dependent on the UAV's dynamics and geometry. This change in channel coefficients motivates

the need to analytically calculate the achievable rate region for multiple access channels in the presence of
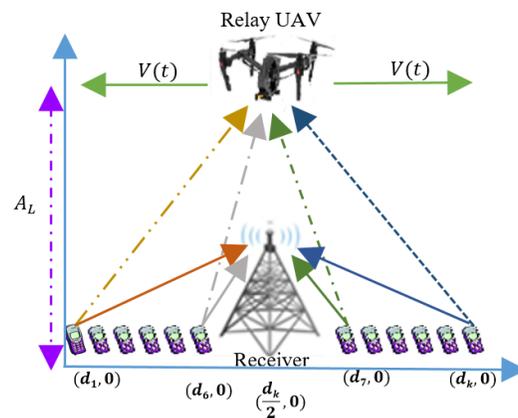
a UAV relay.



Fig. 1. A System With $k$ Terrestrial Transmitters, Terrestrial Receiver, and UAV Relay.

## 1-1- Related works

A number of articles have dealt with calculating the achievable rate region for MAC and MARC.

For instance, the inner bound on the capacity region using decoding techniques and the outer

bound on the capacity region derived via Fano's inequality for a non-causal memoryless MARC

with two terrestrial transmitters and one terrestrial relay are presented in [11]. In [12], the authors

derive achievable rate regions for MARCs with relay–source feedback and show that feedback

enables cooperation among sources by allowing them to resolve residual uncertainty at the

destination. This line of work is further extended in [12] and subsequent studies by incorporating

feedback into both discrete memoryless and Gaussian MARC models. However, these works

primarily focus on feedback-enabled cooperation and do not consider the impact of relay

geometry or air-to-ground propagation characteristics.

The inner and outer bounds on the capacity region for Slepian-Wolf-MARC with two terrestrial

transmitters, one terrestrial receiver, and one terrestrial relay over a discrete memoryless alphabet

are provided in [13], with the results later extended to continuous alphabets. In [14], the authors

propose a partial decode-and-forward strategy for Slepian-Wolf-MARC without memory, calculating the achievable rate region for both discrete and continuous alphabets. Unlike [13, 14], the present work does not assume fading-based opportunistic scheduling or power optimization, but instead focuses on the structural impact of a UAV relay with dominant line-of-sight (LoS) channels.

Fundamental capacity bounds for MARCs are investigated in [15], where outer bounds and achievable strategies such as decode-and-forward, compress-and-forward, and amplify-and-forward are presented for discrete memoryless and Gaussian MARCs. While [15] provides a comprehensive theoretical foundation for MARCs, it does not address scenarios involving aerial relays or phase-dependent channel alignment.

The sum-capacity of degraded Gaussian MARCs is studied in [16], where the authors show that decode-and-forward strategies achieve capacity or sum-capacity under specific degradedness and SNR conditions. This work relies on polymatroid structures arising from terrestrial multiaccess links and does not account for spatial mobility or geometric flexibility of relays.

Achievable rate regions for half-degraded MARCs are considered in [17], where superposition coding and joint decoding strategies are employed, and the results are extended to Gaussian channels. Although this work broadens the class of MARCs under study, it still assumes conventional relay models and does not incorporate UAV-assisted relaying or air-to-ground channel effects.

In contrast to the above works, the present paper investigates a UAV-assisted multiple-access relay channel with a fixed aerial relay, independent transmitters, and LoS-dominated air-to-ground links. The achievable rate region is derived by explicitly accounting for the geometric configuration and phase relationships between the UAV relay and ground nodes, which are not addressed in existing MARC literature.

In [18], the outer bound on the capacity region for Slepian-Wolf-MARC is obtained through relay cooperation, considering correlated noise between the terrestrial relay and two terrestrial transmitters. Reference [19] employs a partial decode-and-forward strategy along with conventional Markov inverse encoding/decoding blocks to calculate the achievable rate region for MARC with and without memory, involving three terrestrial transmitters, one terrestrial receiver, and one terrestrial relay. The energy efficiency of MARC with a common message, two terrestrial transmitters, and one terrestrial relay is investigated in [20]. Additionally, [21] derives the upper bound on the capacity region for a multi-transmitter relay channel using a decode-and-forward strategy with two relays and two receivers. All the aforementioned studies focus on calculating the achievable rate region for channels utilizing terrestrial-based antennas.

As mentioned earlier, the integration of UAVs into modern telecommunication systems offers significant advantages. To leverage this potential, a considerable body of research has focused on optimizing UAV operational parameters in multiple access channels. These studies typically pursue objectives such as increasing data rate or system capacity through trajectory and path optimization [5,22,23], 3D positioning and deployment [24, 25, 26, 27], and joint power control and radio resource allocation [26]. Alongside these core optimization themes, attention to the inherent constraints of UAVs - such as limited energy and processing power - has driven some studies toward designing lightweight solutions, particularly in critical areas like secure and efficient authentication protocols [28, 29, 30]. This category of work aims to minimize computational and communication overhead while ensuring security, thereby enhancing the operational sustainability of UAV-aided networks.

However, to the best of our knowledge and based on our research, the achievable rate region for these systems has not been analytically calculated. Therefore, in the following sections, we will derive the achievable rate region for a Gaussian MARC-UAV (GMARC-UAV) system.

The integration of a UAV as an aerial relay fundamentally redefines the system model compared to terrestrial [11, 13, 14, 18, 19, 21]. While the dominant Line-of-Sight (LoS) component suggests a more deterministic channel, the combined effects of the UAV's mobility, subtle scattering from the environment, and potential hovering instabilities necessitate a slow, flat-fading Rician channel model. This model accurately captures the strong LoS path alongside a weaker random component. Consequently, the channel coefficients are inherently time-variant and spatially dependent, evolving primarily with the UAV's 3D trajectory. This stands in stark contrast to the static channel geometries assumed in terrestrial MARC studies and the Rayleigh fading model typical of non-LoS environments.

The foundational works on MARCs [11, 13, 14, 18, 19, 21] have established rigorous theoretical bounds, but they are confined to a static network paradigm. In these studies, the achievable rate region is a fixed characteristic of a given, unchanging topology. Our work introduces a paradigm shift by leveraging UAV mobility not merely as a feature, but as a core controllable degree of freedom. This transforms the achievable rate region from a static consequence of the network into a dynamic and optimizable function of the UAV's trajectory. Therefore, the principal technical differentiation of our work is the transition from analyzing a fixed capacity region for a given topology to actively shaping and optimizing a spatially/temporally evolving capacity region through strategic trajectory planning a problem domain that remains largely unexplored in the existing MARC literature.

This paradigm shift directly informs our core contribution. We derive the achievable rate region for a Gaussian MARC with a UAV relay, explicitly characterizing it as a function of the relay's spatial coordinates.

**1-2- Research Gaps when terrestrial relays are replaced by UAV relays**

Although the existing literature on multiple-access relay channels (MARCs) provides comprehensive insights into achievable rate regions and capacity bounds with terrestrial relays, several fundamental research gaps arise when the relay is replaced by a UAV-mounted antenna.

a)  First, prior works such as [12, 13, 14, 15, 16, 17] implicitly assume fixed terrestrial relay locations with static channel statistics. When the relay is aerial, the relay–destination and source–relay links exhibit strong geometric dependence, where distance, elevation angle, and relative phase alignment directly affect the achievable rates. These geometric and phase-related effects are not captured in conventional MARC models.

a)  Second, classical MARC formulations typically rely on rich-scattering or fading-based channel models. In contrast, UAV-assisted communications are dominated by line-of-sight (LoS) propagation, leading to fundamentally different channel behaviors, especially in terms of coherent signal combining and phase-sensitive rate regions. Existing terrestrial MARC analyses do not address this LoS-dominated regime.

c)  Third, existing studies focus on cooperation mechanisms enabled by feedback, power allocation, or degradedness assumptions. However, when a UAV relay is employed, the spatial placement of the relay itself becomes a new degree of freedom that influences the structure of the achievable rate region, even when the UAV location is fixed. This spatial dimension is absent in terrestrial relay models.

d)  Fourth, prior MARC capacity results often exploit polymatroid structures arising from conventional multiaccess links. The presence of an aerial relay with phase-aligned channels introduces additional coupling between users' signals that alters the boundary of the rate region, a phenomenon not investigated in existing terrestrial MARC literature.

e)  Finally, most available results are derived for two-user or simplified relay configurations. Extending these results to a general $(k)$-user MARC with a UAV relay and independent transmitters remains largely unexplored.

These gaps motivate the present study, which characterizes the achievable rate region of a (k)-user multiple-access channel assisted by a fixed UAV relay under LoS-dominated air-to-ground propagation.

**1-3- Our contribution**

In this paper: We extend the known rate region for discrete and memoryless -MARC to the continuous alphabet wireless MARC with UAV relay the results of which are necessary for analyzing wireless communication performances. With UAV relay, the wireless region is time varying and hence, is exploitable for improving performances.

**1-4- Paper organization**

The remainder of this paper is structured as follows:

- b)   Section II: System model and notation.
- c)   Section III: Achievable rate region derivation.
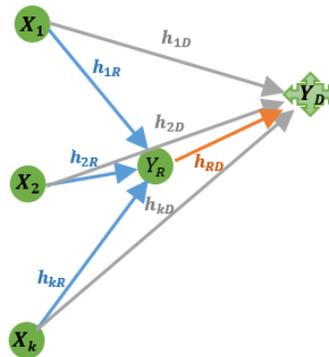- d)   Section IV: Simulation results and conclusions.



Fig. 2. A System Model With $k$ Terrestrial Transmitters, Terrestrial Receiver, and UAV Relay.

**2.  System Model**

This paper uses terrestrial and UAV antennas to calculate the achievable GMARC rate region. Since the UAV motion, location, and type of antenna and users, coding and decoding methods, and channel model affect the rate region, this section discusses the details of the network and system model.

## 2-1- Network model

The multiple-access telecommunications network discussed in this article is depicted Fig.1. As illustrated, the system comprises $k$ terrestrial transmitters and a terrestrial receiver, all positioned along a straight line. If the transmitters are not aligned in a straight line, their relative height with respect to the UAV will vary, leading to changes in the channel coefficients. Consequently, if this assumption is modified, the simulation results must be recalculated based on the updated height values. A UAV relay, flying at a fixed altitude denoted as $A_L$, is deployed above this line. Clearly defining the UAV's movement strategy is essential, as it plays a critical role in determining the achievable rate region of the channel.

In this work, we adopt the movement model proposed [32]. According to this model, the UAV initiates its flight from a position above the first user and moves along the straight line at its maximum speed, $v_{\max}$, until it reaches the last transmitter. Upon reaching the last transmitter, the UAV reverses direction and returns to the first transmitter along the same trajectory. This cyclic movement, characterized by a period $T$, is repeated indefinitely. The UAV's position along the straight line at any time $t$ is described by the function $r(t)$.

Furthermore, we assume the channel coefficients with the UAV relay are deterministic, as the utilization of a UAV in this configuration facilitates strong LoS wireless links. This means that the UAV relay have direct vision, and as mentioned earlier, direct vision causes the channel coefficients to be deterministic. This determinism significantly improves the reliability of communication.

## 2-2- GMARC-UAV

As shown in Fig.2, we consider a specific MARC-UAV channel with a continuous Gaussian alphabet, considering a degraded channel model. In this article, we assumed $k$ terrestrial transmitters and a UAV relay. In this model, transmitters 1 through $k$ generate independent messages $X_1$ through $X_k$. Following the encoding scheme presented [19], each transmitter $i$ partitions its message $X_i$ into two parts: $V_i$ and $U_i$,

which $V_i$ can be decoded at both the relay and the destination and $U_i$ can be decodable only at the destination.

We assume $V_i$ and $U_i$ are independent Gaussian signals, $V_i \sim N(0,1)$ and $U_i \sim N(0,1)$.

Each transmitter $1, 2, \ldots, k$ is subject to an individual power constraint $P_1, P_2, \ldots, P_k$ Let $\gamma_1, \gamma_2, \ldots, \gamma_k$, denote the fractions of the source power allocated to $V_1, V_2, \ldots, V_k$ and $\beta_1, \beta_2, \ldots, \beta_k$ represent the fractions allocated to $U_1, U_2, \ldots, U_k$. Consequently, the transmitted signals $X_1, X_2, \ldots, X_k$ can be expressed as follows:

$$\begin{cases} X_i = \sqrt{\gamma_i P_i} V_i + \sqrt{\beta_i P_i} U_i \\ \gamma_i + \beta_i = 1 \\ i = 1, 2, \ldots, k \end{cases} \quad (1)$$

$$Y_R = \sum_{i=1}^{k} h_{iR}(r(t)) X_i + Z_R$$

Clearly, $X_1, X_2, \ldots, X_k$ are independent Gaussian signals, each distributed as $X_i \sim N(0, P_i)$. In typical scenarios, terrestrial transmitters and receiver often lack a direct LoS between receivers and transmitters. As a result, the channels between them can be modeled as experiencing slow, flat fading with time-invariant stochastic coefficients. Additionally, we account for the presence of AWGN in these channels. As previously mentioned, the UAV benefits from a direct LoS, and thus, the channel coefficients are deterministic, time-variant, and modeled under the assumption of an AWGN channel. The received signal at the relay can be expressed as:

$$Y_R = \sum_{i=1}^{k} h_{iR}(r(t)) X_i + Z_R \quad (2)$$

Here, $h_{iR}(r(t))$, for $i = 1, 2, \ldots, k$, represents the channel coefficient between the transmitter $i$ and the relay. Eq.2, $Z_R \sim N(0, N_{iR})$ denotes the additive white Gaussian noise at the relay.

The relay first receives the signal from the transmitter $i$ and decodes $V_i$. It then codes the decoded message and transmits it to the destination. The relay is subject to a power constraint $P_R$ for transmitting

the signal. Let $\alpha_1, \alpha_2, \ldots, \alpha_k$ denote the portions of $P_R$ allocated to transmitting the encoded signals

$V_1, V_2, \ldots, V_k$ respectively. The UAV relay transmits the following signal to the terrestrial receiver:

$$\begin{cases} X_R = \sum_{i=1}^{k} \sqrt{\alpha_i P_R} V_i \\ \sum_{i=1}^{k} \alpha_i = 1 \qquad (3) \\ X_R \sim N\left(0, P_R\right) \end{cases}$$

Then, the signals sent from transmitters and relay are received by the terrestrial receiver as follows:

$$Y_D = \sum_{i=1}^{k} h_{iD} X_i + Z_R + h_{RD}(r(t)) X_R + Z_D \quad (4)$$

Here, $h_{iD}\$$ represents the channel coefficient between the transmitter $i$ and the terrestrial receiver. These

coefficients are generally random due to the absence of a direct LoS between the transmitters and the

receiver. Since both the transmitters and the receiver are stationary, these coefficients are time-invariant

during message transmission. Additionally, Eq.4, $h_{RD}(r(t))$ denotes the channel coefficient between the

UAV relay and the terrestrial receiver, which is considered deterministic and time varying. Assuming an

AWGN channel, $Z_D \sim N(0, N_D)$ represents the additive Gaussian noise at the receiver.

In the next section, we will derive the achievable rate of the GMARC-UAV system based on Eq.1 – Eq.4.

## 3. Achievable Rate Region

We use the coding and decoding method [19], Decode-and-Forward (DF) strategy, and calculate the

achievable rate region for GMARC-UAV with $k$ transmitters, a UAV relay, and a terrestrial receiver.

Like reference [19], we perceive the messages independently. When we have UAV in channel, the

channel coefficients change over time. In this case to calculate the achievable rate region, we need

calculate the time average.

We calculate the new inner bound on the achievable rate region for Degraded discrete memoryless (DM)

MARC (one transmitter) [31] to $k$ transmitters and UAV relay. We have achievable rate for each

transmitter as follows. For example, $R_{r1}$ is achievable rate between transmitter 1 and relay, and $R_{d1}$ is achievable rate between transmitter 1 and destination.

$$
\begin{cases}
R_{r1}(t) < I\left(X_1 ; Y_R \mid X_R, X_2, \ldots, X_k, V_1, V_2, \ldots V_k\right) \\
R_{rk}(t) < I\left(X_k ; Y_R \mid X_R, X_1, X_2, \ldots, X_{k-1}, V_1, V_2, \ldots V_k\right) \\
\sum_{i=1}^{k} R_{ri}(t) < I\left(X_1, X_2, \ldots, X_k ; Y_R \mid X_R, V_1, V_2, \ldots V_k\right)
\end{cases} \quad (5)
$$

Also, the achievable rate in the receiver is:

$$
\begin{cases}
R_{d1}(t) < I\left(X_1, X_R ; Y_D \mid X_2, \ldots, X_k, V_2, V_3, \ldots V_k\right) \\
R_{dk}(t) < I\left(X_k, X_R ; Y_D \mid X_1, X_2, \ldots, X_{k-1}, V_1, V_2, \ldots V_{k-1}\right) \\
\sum_{i=1}^{k} R_{di}(t) < I\left(X_1, X_2, \ldots, X_k, X_R ; Y_D\right)
\end{cases} \quad (6)
$$

where, $I(.\ ;\ .\mid.)$ represents conditional mutual information.

In the presented system model, where the UAV serves as the receiver, it is crucial to recognize that the UAV's spatial position and corresponding channel coefficients vary over time. This temporal variation leads to time-dependent modifications in the achievable rate region. Consequently, all equation parameters become functions of time, transforming the achievable rate region expressions as follows:

    a)   Compute the time average of the instantaneous rate expressions given Eq.5, Eq.6.

    b)   Select the minimum values following multi-user information theory principles

Then the achievable rate region in the channel is $min[(5),(6)]$ and time average in UAV relay, as below:

$$
\begin{cases}
R_1 < \min\left(R_{r1}, R_{d1}\right) \\
R_k < \min\left(R_{rk}, R_{dk}\right) \\
\sum_{i=1}^{k} R_i < \min\left(\sum_{i=1}^{k} R_{ri}, \sum_{i=1}^{k} R_{di}\right)
\end{cases} \quad (7)
$$

Where, $R_i$, $R_{rk}$, and $R_{dk}$ respectively, are the rate of channel, relay and transmitter $i$.

Therefore, the distance between UAV and transmitters is a function of time and depends on the scenario of the UAV movement. We perceive the motion scenarios [32] and calculate the distance, channel coefficients, and achievable rate region in the GMARC-UAV with the system model in the previous section.

According to Eq.1, Eq.2, Eq.3, Eq.5 and time average in UAV relay, the achievable rate region in the relay, is as follows:

$$
\begin{aligned}
R_{r1}(t) &< I\left(X_1; Y_R \mid X_R, X_2, \ldots, X_k, V_1, V_2, \ldots V_k\right) = H\left(Y_R \mid X_R, X_2, \ldots, X_k, V_1, V_2, \ldots V_k\right) - H\left(Y_R \mid X_1, X_R, X_2, \ldots, X_k, V_1, V_2, \ldots V_k\right) \\
&= H\left(\sum_{i=1}^{k} h_{iR}(r(t)) X_i + Z_R \mid X_R, X_2, \ldots, X_k, V_1, V_2, \ldots V_k\right) - H\left(\sum_{i=1}^{k} h_{iR}(r(t)) X_i + Z_R \mid X_1, X_R, X_2, \ldots, X_k, V_1, V_2, \ldots V_k\right) \\
&= H\left(h_{1R}(r(t)) X_1 + Z_R \mid X_R, X_2, \ldots, X_k, V_1, V_2, \ldots V_k\right) - H\left(Z_R\right) = H\left(h_{1R}(r(t))\sqrt{\beta_1 P_1} U_1 + Z_R \mid X_R, X_2, \ldots, X_k, V_1, V_2, \ldots V_k\right) - H\left(Z_R\right) \\
&= \frac{1}{T}\int_0^T \frac{1}{2}\log\left(2\pi e\left(N_R + \left(h_{1R}(r(t))\sqrt{\beta_1 P_1} U_1\right)^2\right)\right) dt - \frac{1}{2}\log\left(2\pi e N_R\right) = \frac{1}{T}\int_0^T \frac{1}{2}\log\left(1 + \frac{|h_{1R}(r(t))|^2 \beta_1 P_1}{N_R}\right) dt
\end{aligned}
\tag{8}
$$

Also, such as (8) we have:

$$
\begin{cases}
R_{r2} < \dfrac{1}{T}\displaystyle\int_0^T \dfrac{1}{2}\log\left(1 + \dfrac{|h_{2R}(r(t))|^2 \beta_2 P_2}{N_R}\right) dt \\
\;\vdots \\
R_{rk} < \dfrac{1}{T}\displaystyle\int_0^T \dfrac{1}{2}\log\left(1 + \dfrac{|h_{1R}(r(t))|^2 \beta_1 P_1}{N_R}\right) dt
\end{cases}
\tag{9}
$$

We will calculate $\sum_{i=1}^{k} R_{ri}$ such as $R_{r1}$:

$$
\begin{aligned}
\sum_{i=1}^{k} R_{ri}(t) &< I\left(X_1, X_2, \ldots, X_k; Y_R \mid X_R, V_1, V_2, \ldots V_k\right) = H\left(Y_R \mid X_R, V_1, V_2, \ldots V_k\right) - H\left(Y_R \mid X_R, X_1, X_2, \ldots, X_k, V_1, V_2, \ldots V_k\right) \\
&= H\left(\sum_{i=1}^{k} h_{iR}(r(t)) X_i + Z_R \mid X_R, V_1, V_2, \ldots V_k\right) - H\left(\sum_{i=1}^{k} h_{iR}(r(t)) X_i + Z_R \mid X_R, X_1, X_2, \ldots, X_k, V_1, V_2, \ldots V_k\right) \\
&= H\left(\sum_{i=1}^{k} h_{iR}(r(t))\left(\sqrt{\gamma_i P_i} V_i + \sqrt{\beta_i P_i} U_i\right) + Z_R \mid X_R, V_1, V_2, \ldots V_k\right) - H\left(Z_R\right) = H\left(\sum_{i=1}^{k} h_{iR}(r(t))\sqrt{\beta_i P_i} U_i + Z_R\right) - H\left(Z_R\right) \\
&= \frac{1}{T}\int_0^T \frac{1}{2}\log\left(2\pi e\left(\sum_{i=1}^{k}\left(h_{iR}(r(t))\sqrt{\beta_i P_i}\right)^2 + N_R\right)\right) dt - \frac{1}{2}\log\left(2\pi e N_R\right) = \frac{1}{T}\int_0^T \frac{1}{2}\log\left(1 + \frac{|h_{iR}(r(t))|^2 \beta_i P_i}{N_R}\right) dt
\end{aligned}
\tag{10}
$$

According to Eq.1, Eq.3, Eq.4, Eq.6, the achievable rate region in the receiver, is as follows:

$$R_{d1}(t) < I\left(X_1, X_R; Y_D \mid X_2,...,X_k, V_2, V_3,..V_k\right) = H\left(Y_D \mid X_2,...,X_k, V_2, V_3,..V_k\right) - H\left(Y_D \mid X_R, X_1, X_2,...,X_k, V_2, V_3,..V_k\right)$$

$$= H\left(\sum_{i=1}^{k} h_{iD} X_i + Z_R + h_{RD}(r(t)) X_R + Z_D \mid X_2,...,X_k, V_2, V_3,..V_k\right) - H\left(Z_D + Z_R\right)$$

$$= H\left(h_{1D} X_1 + Z_R + h_{RD}(r(t)) X_R + Z_D \mid V_2, V_3,..V_k\right) - H\left(Z_D + Z_R\right)$$

$$= H\left(h_{1D}\left(\sqrt{\gamma_1 P_1} V_1 + \sqrt{\beta_1 P_1} U_1\right) + Z_R + h_{RD}(r(t))\sum_{i=1}^{k}\sqrt{\alpha_i P_R} V_i + Z_D \mid V_2, V_3,..V_k\right) - H\left(Z_D + Z_R\right)$$

$$= H\left(h_{1D}\sqrt{\beta_1 P_1} U_1 + Z_R + \left(h_{1D}\sqrt{\gamma_1 P_1} + h_{RD}(r(t))\sqrt{\alpha_1 P_R}\right) V_1 + Z_D \mid V_2, V_3,..V_k\right) - H\left(Z_D + Z_R\right)$$

$$= \frac{1}{T}\int_0^T \frac{1}{2}\log\left(2\pi e\left(N_D + |h_{1D}|^2 \beta_1 P_1 + |h_{RD}(r(t))|^2 \alpha_1 P_R + |h_{1D}|^2 \gamma_1 P_1 + 2h_{1D}h_{RD}(r(t))\sqrt{P_1 P_R \alpha_1 \gamma_1}\cos\Delta\theta_1\right)\right)dt$$

$$- \frac{1}{2}\log\left(2\pi e\left(N_R + N_D\right)\right) = \frac{1}{T}\int_0^T \frac{1}{2}\log\left(2\pi e\left(1 + \frac{|h_{1D}|^2 \beta_1 P + |h_{RD}(r(t))|^2 \alpha_1 P_R + |h_{1D}|^2 \gamma_1 P_1 + 2h_{1D}h_{RD}(r(t))\sqrt{P_1 P_R \alpha_1 \gamma_1}\cos\Delta\theta_1}{N_R + N_D}\right)\right)dt$$

(11)

We know $\Delta\theta_1$ is the angle between $h_{RD}$ and $h_{1D}$.

Also, we have $R_{dk}$ such as $R_{d1}$:

$$R_{dk} < \frac{1}{T}\int_0^T \frac{1}{2}\log\left(2\pi e\left(1 + \frac{|h_{kD}|^2 \beta_k P_k + |h_{RD}(r(t))|^2 \alpha_k P_R + |h_{kD}|^2 \gamma_k P_k + 2h_{kD}h_{RD}(r(t))\sqrt{P_k P_R \alpha_k \gamma_k}\cos\Delta\theta_k}{N_R + N_D}\right)\right)dt$$ (12)

We will calculate $\sum_{i=1}^{k} R_{di}$ such as $R_{d1}$:

$$\sum_{i=1}^{k} R_{di}(t) < I\left(X_1, X_2,...,X_k, X_R; Y_D\right) = H\left(Y_D\right) - H\left(Y_D \mid X_1, X_2,...,X_k, X_R\right) = H\left(\sum_{i=1}^{k} h_{iD} X_i + Z_R + h_{RD}(r(t)) X_R + Z_D\right) - H\left(Z_R + Z_D\right)$$

$$= H\left(\sum_{i=1}^{k} h_{iD}\left(\sqrt{\gamma_i P_i} V_i + \sqrt{\beta_i P_i} U_i\right) + Z_R + h_{RD}(r(t))\sum_{i=1}^{k}\sqrt{\alpha_i P_R} V_i + Z_D\right) - H\left(Z_R + Z_D\right)$$

$$= H\left(\sum_{i=1}^{k} h_{iD}\sqrt{\beta_i P_i} U_i + Z_R + \left(\sum_{i=1}^{k}\left(h_{iD}\sqrt{\gamma_i P_i} + h_{RD}(r(t))\sqrt{\alpha_i P_R}\right)V_i\right) + Z_D\right) - H\left(Z_R + Z_D\right)$$

$$= \frac{1}{T}\int_0^T \frac{1}{2}\log\left(2\pi e\left(N_D + N_R + \sum_{i=1}^{k}\left(P_i\left(\gamma_i\beta_i\right)|h_{iD}|^2 + |h_{RD}(r(t))|^2 P_R\alpha_i\right) + 2h_{iD}h_{RD}(r(t))\sqrt{P_i P_R \alpha_i \gamma_i}\cos\Delta\theta_i\right)\right)dt - \frac{1}{2}\log\left(2\pi e\left(N_R + N_D\right)\right)$$

$$= \frac{1}{T}\int_0^T \frac{1}{2}\log\left(2\pi e\left(1 + \frac{\sum_{i=1}^{k}\left(P_i\left(\gamma_i\beta_i\right)|h_{iD}|^2 + |h_{RD}(r(t))|^2 P_R\alpha_i\right) + 2h_{iD}h_{RD}(r(t))\sqrt{P_i P_R \alpha_i \gamma_i}\cos\Delta\theta_i}{N_R + N_D}\right)\right)dt$$

(13)

Finally, the achievable rate region in the GMARC-UAV is as follows:

$$\begin{cases} R_k < \min\left(\frac{1}{T}\int_0^T \frac{1}{2}\log\left(1 + \frac{|h_{kR}(r(t))|^2 \beta_k P_k}{N_R}\right)dt, \frac{1}{T}\int_0^T \frac{1}{2}\log\left(2\pi e\left(1 + \frac{|h_{kD}|^2 P_k + |h_{RD}(r(t))|^2 \alpha_k P_R + 2h_{kD}h_{RD}(r(t))\sqrt{P_k P_R \alpha_k \gamma_k}\cos\Delta\theta_k}{N_R + N_D}\right)\right)dt\right) \\ \sum_{i=1}^{k} R_i < \min\left(\frac{1}{T}\int_0^T \frac{1}{2}\log\left(1 + \frac{\sum_{i=1}^{k}|h_{iR}(r(t))|^2 \beta_i P_i}{N_R}\right)dt, \frac{1}{T}\int_0^T \frac{1}{2}\log\left(2\pi e\left(1 + \frac{\sum_{i=1}^{k}|h_{iD}|^2 P_i + |h_{RD}(r(t))|^2 \alpha_i P_R + 2h_{iD}h_{RD}(r(t))\sqrt{P_i P_R \alpha_i \gamma_i}\cos\Delta\theta_i}{N_R + N_D}\right)\right)dt\right) \end{cases}$$

(14)

## 4- Simulations And Results

In this section:

a) We first simulated the achievable rate region for a MARC-UAV system with $k$ (14) terrestrial transmitters and independent Gaussian signals, and a UAV receiver with white Gaussian noise.

b) In the next step, we used the channel coefficients [32], for $h_{iR}(\mathrm{r(t)})$ and $h_{RD}(\mathrm{r(t)})$ (15).

c) We removed the relay and calculate achievable rate region GMAC-UAV (in this case, the transmitters and receiver are terrestrial).

d) Then, we assumed terrestrial relay and used coefficients channel [19], for $h_{iD}$.

e) Then achievable rate region of GMARC-UAV, GMAC-UAV, and terrestrial GMRAC are compared.

Reference [32] we have:

$$h_i(t) = \frac{\lambda}{4\pi d_i(t)} \quad (15)$$

Where:

$$\begin{cases} \lambda = \dfrac{C}{f} \\ d_i(t) = \sqrt{\| d(r(t)) - W_i \|^2 + A_L^2} \\ W_i = \begin{cases} 0 \\ d \end{cases} \end{cases} \quad (16)$$

Also, we deem:

$A_L = 250\ m,\ V_{max} = 20\ ^m/_S,\ P_1 = P_2 = P_R = 30\ dBm,\ N_R = N_D = 10^{-7},\ T = 100\ s,\ \gamma_i = \beta_i = 0.5,\ h_{ir} = 1.6,$

$\alpha_i = \frac{1}{k},\ f = 1.2 GH.$

The notation of this coefficients channel is shown in Table 1.

Table 1. Notation of coefficients channel UAV.

| Notation | Corresponding Meaning |
|---|---|
| $\lambda$ | Wavelength |
| $C$ | Speed of light |
| $d(r(t))$ | Horizontal location of terrestrial transmitter k |
| $A_L$ | UAV's flight altitude |
| $d_i(t)$ | Distance between the UAV and transmitter k at time t |
| $h_i(r(t))$ | Channel power gain between the UAV and transmitter k at time t |
| $h_{ir}$ | Channel power gain between the terrestrial antenna and transmitter k |

We put Eq.15 and Eq.16 in Eq.14, and performed the simulation in the MATLAB (GMARC-UAV). If we

delete parameters of relay, the Eq.14 is changed to:

$$R_1 < \frac{1}{2}\log\left(2\pi e\left(1+\frac{P_1\,|\,h_{1D}\,|^2}{N_D}\right)\right) \quad (17)$$

$$R_k < \frac{1}{2}\log\left(2\pi e\left(1+\frac{P_k\,|\,h_{kD}\,|^2}{N_D}\right)\right) \quad (18)$$

$$\sum_{i=1}^{k}R_i < \frac{1}{2}\log\left(2\pi e\left(1+\frac{\sum_{i=1}^{k}P_i\,|\,h_{iD}\,|^2}{N_D}\right)\right) \quad (19)$$

We used Eq.17- Eq.19 to simulate achievable rate region MARC in MATLAB. If we assume a terrestrial

relay, we have:

$$\begin{cases} R_k < \min\left(\frac{1}{T}\int_0^T\frac{1}{2}\log\left(1+\frac{|\,h_{kR}(r(t))\,|^2\,\beta_k P_k}{N_R}\right)dt,\frac{1}{T}\int_0^T\frac{1}{2}\log\left(2\pi e\left(1+\frac{|\,h_{kD}\,|^2\,P_k+|\,h_{RD}(r(t))\,|^2\,P_R+2h_{kD}h_{RD}(r(t))\sqrt{P_k P_R \alpha_k \gamma_k}\,\cos\Delta\theta_k}{N_R+N_D}\right)\right)dt\right) \\[2ex] \sum_{i=1}^k R_i < \min\left(\frac{1}{T}\int_0^T\frac{1}{2}\log\left(1+\frac{\sum_{i=1}^k|\,h_{iR}(r(t))\,|^2\,\beta_i P_i}{N_R}\right)dt,\frac{1}{T}\int_0^T\frac{1}{2}\log\left(2\pi e\left(1+\frac{\sum_{i=1}^k|\,h_{iD}\,|^2\,P_i+|\,h_{RD}(r(t))\,|^2\,P_R+2h_{iD}h_{RD}(r(t))\sqrt{P_i P_R \alpha_i \gamma_i}\,\cos\Delta\theta_i}{N_R+N_D}\right)\right)dt\right) \end{cases} \quad (20)$$

We utilized Eq.20 to simulate the achievable rate region of a MARC with a terrestrial relay in MATLAB.

The results, depicted in Fig.3, demonstrate that the inclusion of the relay significantly enhances the

achievable rate region. Furthermore, transitioning the relay from a terrestrial antenna to an UAV does not diminish the achievable rate region. However, it is noteworthy that employing UAV relays introduces LoS conditions, where the channel coefficients become deterministic and time-variant. This characteristic facilitates the estimation of channel coefficients and simplifies the practical realization of the achievable rate region.

Due to the direct LoS between the relay and the receiver and transmitters, the channel coefficient is non-random and, in many cases, exceeds the coefficient of the terrestrial antennas which are random and the achievable rate region increases. The result is shown in Fig.3.
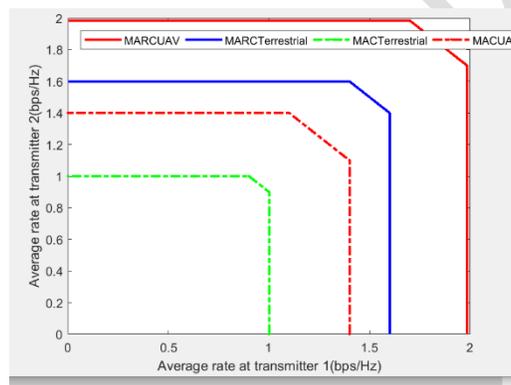


Fig. 3. Comparison of the achievable rate regions.

If direct LoS between the relay and the receiver and transmitters is Changed to non LoS(NLos), the achievable rate region is decrease (like terrestrial antenna). Fig.4, demonstrate that the inclusion of the relay significantly enhances the achievable rate region with decrementation channel coefficients in NLoS.
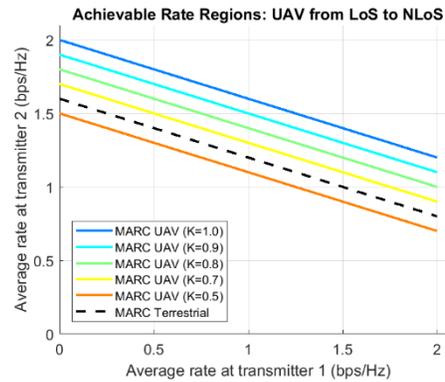
Fig. 4. Comparison of the achievable rate regions between LoS and NLoS.

**4- Conclusion**

In this paper, we first extended the known rate region for DMC-MARC to the continuous alphabet version of wireless MARC with a UAV relay. Then, we calculated the obtained achievable rate region for the MARC with a UAV relay, involving $k$ transmitters and a terrestrial receiver, by simulating the channel conditions. The simulation results indicate that the introduction of a relay significantly expands the achievable rate region of the channel.

**References**

[1] Bouziane Brik, Adlen Ksentini, Maha Bouaziz, "Federated Learning for UAVs-Enabled Wireless Networks: Use Cases, Challenges, and Open Problems",IEEE access, Vol 8,pp 53841 – 53849, March 2020, 10.1109/ACCESS.2020.2981430.

[2] Dongfang Xu, Yan Sun, Derrick Wing Kwan Ng, Robert Schober, "Multiuser MISO UAV Communications in Uncertain Environments with No-Fly Zones: Robust Trajectory and Resource Allocation Design", IEEE Transactions On Communications, vol 68, NO. 5, May 2020, 10.1109/TCOMM.2020.2970043.

[3] Dingkun Hu, Qi Zhang, Quanzhong Li, Jiayin Qin, "Joint Position, Decoding Order, and Power Allocation Optimization in UAV-Based NOMA Downlink Communications", IEEE Systems Journal, Vol 14, Iss 2, June 2020, 10.1109/JSYST.2019.2940985.

[4] Shuhang Zhang, Hongliang Zhang, Boya Di, Lingyang Song, "Cellular UAV-to-X Communications: Design and Optimization for Multi-UAV Networks", IEEE Transactions on Wireless Communications, Vol 18, Iss 2, February 2019, 10.1109/TWC.2019.2892131.

[5] Peiming Li, Jie Xu, "Fundamental Rate Limits of UAV-Enabled Multiple Access Channel with Trajectory Optimization", IEEE Transactions on Wireless Communications, Vol 19, no 1, January 2020, 10.1109/TWC.2019.2946153.

[6] Amir Masoud Aminian-Modarres, Mohammad Molavi-Kakhki. "A nonlinear signal processing method for diversity combining using Hammerstein type filter." International Journal of Computer Science and Network Security, vol. 9, no. 1 (2009): 399-407.

[7] Amir Masoud Aminian-Modarres, Mohammad Molavi-Kakhki. "A nonlinear equalization technique for frequency selective fading channels." In 2009 IEEE International Conference on Signal and Image Processing Applications, pp. 369-373. IEEE, 2009, doi: 10.1109/icsipa.2009.5478679.

[8] Amir Masoud Aminian-Modarres, Mohammad Molavi-Kakhki. "A Hammerstein diversity combining technique." International Journal of Information and Communication Technology Research, vol. 2, no. 1, (2010): 53-63.

[9] Amir Masoud Aminian-Modarres, Mohammad Molavi-Kakhki. "A Blind Hammerstein Diversity Combining Technique for Flat Fading Channels." International Journal of Engineering, vol. 26, no. 3, (2013): 277-288, doi: 10.5829/idosi.ije.2013.26.03c.07.

[10] Amir Masoud Aminian-Modarres, Mohammad Molavi-Kakhki, Amir Reza Momen. "Investigating the effects of different fading channels on the performance of generalized Hammerstein equalization technique." In 6th International Symposium on Telecommunications (IST), pp. 322-327. IEEE, 2012, doi: 10.1109/istel.2012.6483005.

[11] Mohammad Osmani-Bojd, Ghosheh Abed Hodtani, "Multiple-access relay channels with non-causal channel state information at the relay", Transactions on Emerging Telecommunications Technologies, Vol. 28, Iss. 1, November 2014, 10.1002/ett.2900

[12] Hou, Jie, Ralf Koetter, and Gerhard Kramer. "Rate regions for multiple access relay channels with relay-source feedback." 2009 IEEE Information Theory Workshop. IEEE, 2009.

[13] Ehsan Moeen Taghavi, Ghosheh Abed Hodtani, "Multiple Access Relay Channel with Relay-Sources Feedback", IEEE. Translations and content mining IEEE Access, Vol 6, July 2018, 10.1109/ACCESS.2018.2865501.

[14] Ehsan Moeen Taghavi Ghosheh Abed Hodtani, "Partial feedback impact on achievable rate region in multiple-access relay channels", International journal of communication systems, Vol 31, Iss 17, August 2018, 10.1002/dac.3807.

[15] Sankar, Lalitha, et al. "Fading multiple access relay channels: Achievable rates and opportunistic scheduling." IEEE Transactions on Information Theory 57.4 (2011): 1911-1931.

[16] Sankaranarayanan, Lalitha, Gerhard Kramer, and Narayan B. Mandayam. "Capacity theorems for the multiple-access relay channel." Allerton Conference on Communication, Control, and Computing. 2004.

[17] Sahebalam, Assadallah, Mohammad Osmani-Bojd, and Ghosheh Abed Hodtani. "Achievable rate regions for multiple-access half-degraded relay channels." ICTC 2011. IEEE, 2011.

[18] A. Sahebalam, M. Osmani-Bojd, G. A. Hodtani, "Ultra-wideband multiple-access relay channel with correlated noises and its diversity analysis", International Journal Of Communication Systems, vol 28, iss 7, May 2015,10.1002/dac.2753 7.

[19] Ehsan Moeen Taghavi, Ghosheh Abed Hodtani, "Impact of the relay on the coverage region of multiple-access channels, Institution of Engineering and Technology", vol 10, iss 5, March 2016, 10.1049/iet-com.2015.0685

[20] Ehsan Moeen Taghavi, Ghosheh Abed Hodtani, "Energy efficient communications over multiple access relay channels", International journal of communication systems, Vol 30, Iss 18, June 2017, 10.1002/dac.3368

[21] Antony V. Mampilly, Srikrishna Bhashyam ,"Successive Relaying for Two-hop Two-Destination Multicarrier Relay Channels", IEEE Communications Letters, Vol 24, Iss 3, March 2020, 10.1109/LCOMM.2020.2964243.

[22] JeiHee Cho,SooMin Ki,HyungJune Lee, "Predictive Path Planning of Multiple UAVs for Effective Network Hotspot Coverage", IEEE Transactions on Vehicular Technology, pp.1-16 July 2023, 10.1109/TVT.2023.3299302.

[23] Jiehong Wu,Ya'nan Sun,Danyang Li,Junling Shi,Xianwei Li,Lijun Gao,Lei Yu,Guangjie Han,Jinsong Wu, "An Adaptive Conversion Speed Q-Learning Algorithm for Search and Rescue UAV Path Planning in Unknown Environments", IEEE Transactions on Vehicular Technology, pp.1-14 July 2023, 10.1109/TVT.2023.3297837.

[24] Yujae Song, Sung Hoon Lim, Sang-Woon Jeon, Seungjae Baek, "On Cooperative Achievable Rates of UAV Assisted Cellular Networks", IEEE Transactions On Vehicular Technology, VOL. 0, NO. 0, JUNE 2020, 10.1109/TVT.2020.3003301.

[25] Nikita Tafintsev,Dmitri Moltchanov,Alessandro Chiumento,Mikko Valkama,Sergey Andreev, "Airborne Integrated Access and Backhaul Systems: Learning-Aided Modeling and Optimization", IEEE Transactions on Vehicular Technology, pp.1-14 July 2023, 10.1109/TVT.2023.3293171.

[26] Asad Mahmood,Thang X. Vu,Symeon Chatzinotas,Björn Ottersten, "Joint Optimization of 3D Placement and Radio Resource Allocation for per-UAV Sum Rate Maximization", IEEE Transactions on Vehicular Technology, pp.1-12, May 2023, 10.1109/TVT.2023.3274815.

[27] Yuhan Su,Minghui Liwang,Zhong Chen,Xiaojiang Du, "Toward Optimal Deployment of UAV Relays in UAV-Assisted IoV Networks", IEEE Transactions on Vehicular Technology, pp.1-14, May 2023, 10.1109/TVT.2023.3272648.

[28] Modarres, Amir Masoud Aminian, and Ghazaleh Sarbishaei. "Enhancing internet of drones security: A robust multi-factor authentication and key establishment protocol." IEEE Transactions on Vehicular Technology (2025), doi: 10.1109/TVT.2025.3591497.

[29] Kharghani, Elaheh, et al. "A lightweight authentication protocol for M2M communication in IIoT using physical unclonable functions." 2023 31st International Conference on Electrical Engineering (ICEE). IEEE, 2023, doi: 10.1109/ICEE59167.2023.10334808.

[30] Modarres, Amir Masoud Aminian, and Ghazaleh Sarbishaei. "An improved lightweight two-factor authentication protocol for IoT applications." IEEE transactions on industrial informatics 19.5 (2022): 6588-6598, doi: 10.1109/TII.2022.3201971.

[31] Gamal, A.E, Zahedi, S, "Capacity of a class of relay channels with orthogonal components", IEEE Trans. Information Theory, 2005, 51, (3).

[32] Yi Liu, Ming Qiu, Jinlei Hu, Huimin Yu,"Incentive UAV-Enabled Mobile Edge Computing Based on Microwave Power Transmission, IEEE Access, vol 8, 2020, 10.1109/ACCESS.2020.2971962.